

Influence of Pore Size on the van der Waals Interaction in Two-Dimensional Molecules and Materials

Yan Yang, Ka Un Lao, and Robert A. DiStasio, Jr.*

Department of Chemistry and Chemical Biology, Cornell University, Ithaca, New York 14853, USA

 (Received 2 July 2018; revised manuscript received 9 October 2018; published 14 January 2019)

Despite the importance of porous two-dimensional (2D) molecules and materials in advanced technological applications, the question of how the void space in these systems affects the van der Waals (vdW) scaling landscape has been largely unanswered. Analytical and numerical models presented herein demonstrate that the mere presence of a pore leads to markedly different vdW scaling across nonasymptotic distances, with certain relative pore sizes yielding effective power laws ranging from simple monotonic decay to the formation of minima, extended plateaus, and even maxima. These models are in remarkable agreement with first-principles approaches for the 2D building blocks of covalent organic frameworks (COFs), and reveal that COF macrocycle dimers and periodic bilayers exhibit unique vdW scaling behavior that is quite distinct from their nonporous analogs. These findings extend across a range of distances relevant to the nanoscale, and represent a hitherto unexplored avenue towards governing the self-assembly of complex nanostructures from porous 2D molecules and materials.

DOI: [10.1103/PhysRevLett.122.026001](https://doi.org/10.1103/PhysRevLett.122.026001)

Two-dimensional (2D) materials like graphene, hexagonal boron nitride, and transition metal dichalcogenides have been under intense research for the past decade due to their favorable electronic, optical, thermal, mechanical, and biological properties [1–5]. Allowing for variable pore sizes beyond the atomic dimensions in graphene, porous materials such as covalent organic frameworks (COFs) [6–12], metal organic frameworks [13,14], and porous coordination polymers [15,16] are endowed with additional properties like permanent porosities, high aspect ratios, and large internal surface areas. As such, these materials have led to numerous technological applications, including (opto-)electronics [17], (photo-)thermal devices [18], energy storage materials [19], (bio-)chemical sensors and filters [19,20], size-selective catalysts [21], and even drug delivery vectors [22,23].

The assembly of 2D materials into sophisticated single-layer heterostructures [24] and/or multilayered architectures [including van der Waals (vdW) heterostructures [25–28]], provides access to even more diverse functionalities, targeted properties, and applications. While the monolayers in 2D materials are mostly formed *via* strong covalent bonds, vdW (dispersion) interactions are the predominant forces between the layers. In fact, these ubiquitous forces are largely responsible for self-assembly, and play a crucial role in determining the structure, stability, and function of systems throughout chemistry, physics, and materials science [29–32]. Arising from nonlocal electrodynamic correlations between instantaneous charge fluctuations in matter, vdW interactions are quantum mechanical in nature with an influence that spans distances (D) ranging from atomic dimensions

(i.e., a few Å) to well beyond the nanoscale [33–35]. At these distances, dimensionality, local response properties, and topology—such as the presence of a pore—can strongly influence the strength and scaling of these forces [36,37], and hence the observed system properties.

While analytic vdW scaling laws (such as D^{-5} or D^{-4} for two parallel insulating wires or plates) are central to our understanding of infinite-size systems at asymptotic distances, rather unusual power laws have been observed in both finite and extended systems at intermediate distances relevant to the nanoscale [37–45]. For example, Gould *et al.* [38] argued that the binding energy of graphite varies as D^{-4} for nonasymptotic interlayer separations, which differs from the asymptotic D^{-3} behavior analytically demonstrated by Dobson and co-workers [38,46,47]; this was later confirmed by high-level quantum mechanical calculations [39,41], which found $D^{-4.2}$ for $D \approx 3\text{--}9$ Å. For C_{60} interacting with graphene and a carbon nanotube, Dappe *et al.* [40] observed D^{-3} and $D^{-3.5}$ scaling behavior, respectively, at distances shorter than the C_{60} diameter, in stark contrast to their D^{-4} and D^{-5} asymptotes. Topologically speaking, this example demonstrates that void space has a profound influence over the vdW scaling in these systems, and governs the length scales over which one observes deviations from asymptotic behavior. Since even slight variations in these power laws can markedly impact properties and functionalities, such unusual intermediate-range scaling behavior demands further theoretical investigation.

Despite the importance of porous 2D building blocks in the discovery and development of advanced materials, the

question of how void space—provided here by variable pore sizes ranging from a few Å to 10s of nm—affects the vdW interaction has been less studied. In this Letter, we present analytical and numerical results that demonstrate how variable pore sizes fundamentally alter the vdW scaling landscape in three prototypical model systems representing an atom and a porous macrocycle, a porous macrocycle dimer, and a porous periodic bilayer. We find that certain pore sizes lead to rather unexpected behavior at short and intermediate distances, and the degree and extent to which these deviations differ from asymptotic behavior can be tuned by varying the relative size and shape of these void spaces. When applied to a number of popular COF building blocks, we find that these simple models are in remarkable agreement with first-principles based vdW methods, and reveal that such systems exhibit unique vdW scaling behavior across a range of distances (10–100 Å) quite relevant to the self-assembly of complex nanostructures [48,49].

Throughout this work we quantify the scaling of the vdW interaction energy E_{vdW} between two objects separated by a distance D_{AB} through the effective power law exponent $P_{\text{vdW}}(D)$, defined as [37]

$$P_{\text{vdW}}(D) = \left(\frac{\partial \ln |E_{\text{vdW}}(D_{AB})|}{\partial \ln D_{AB}} \right) \Big|_{D_{AB}=D}. \quad (1)$$

As such, $P_{\text{vdW}}(D)$ provides an effective measure of the $E_{\text{vdW}}(D)$ decay rate and delineates the length scales over which the system deviates from asymptotic behavior. We begin by considering a point particle A separated by D from the center of an annulus with inner and outer radii r and R as a model for the interaction of an atom with a porous macrocycle (Fig. 1). To investigate the vdW scaling behavior in this prototypical model system, we analytically derive $P_{\text{vdW}}^{A\text{-ann}}$

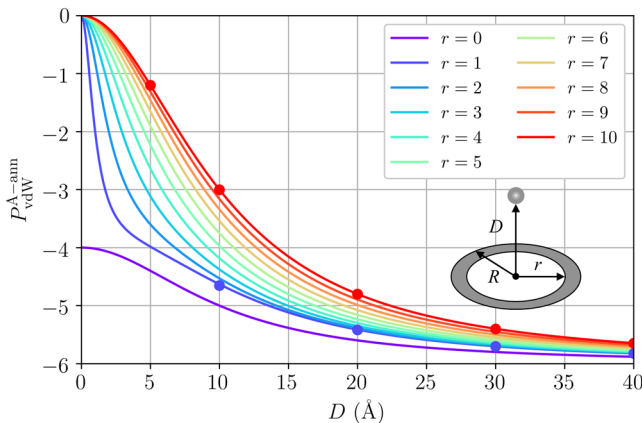


FIG. 1. Effective power law exponents $P_{\text{vdW}}^{A\text{-ann}}$ for the pairwise (lines) and many-body (circles) vdW interaction between a point particle and an annulus with $R = 10$ as a function of r and D (all in Å). The mere presence of a pore fundamentally alters the vdW scaling landscape and leads to a markedly slower $E_{\text{vdW}}^{A\text{-ann}}$ decay rate across all nonasymptotic distances.

based on a second-order perturbative (pairwise) treatment of E_{vdW} and compare our findings to an infinite-order many-body expansion of E_{vdW} via the adiabatic-connection fluctuation-dissipation theorem (ACFDT). Assuming that the annulus (denoted by $\text{ann}[r, R]$) is continuous and insulating, comprised of a single atom type, and located outside of density overlap with A , the pairwise $E_{\text{vdW}} = -\sum_B C_6^{AB} R_{AB}^{-6}$ can be computed by integrating over all annulus surface elements $d\sigma_B$ located at a distance R_{AB} from A , i.e.,

$$E_{\text{vdW}}^{A\text{-ann}}(r, R, D) = -\frac{C_6^{AB}}{S_B} \int d\sigma_B R_{AB}^{-6}, \quad (2)$$

wherein $S_B = \int d\sigma_B$ is the annulus surface area. This integral can be analytically evaluated using cylindrical coordinates to yield $P_{\text{vdW}}^{A\text{-ann}}(r, R, D) = -4/[1 + (r/D)^2] - 4/[1 + (R/D)^2] + 4/[2 + (r/D)^2 + (R/D)^2]$, which is plotted as a function of r and D for $\text{ann}[r, R = 10 \text{ Å}]$ in Fig. 1.

For $r = 0$, the annulus becomes a closed (nonporous) disk and $P_{\text{vdW}}^{A\text{-disk}}(R, D) = P_{\text{vdW}}^{A\text{-ann}}(0, R, D) = -4 - 4/[1 + (R/D)^2] + 4/[2 + (R/D)^2]$. In the short range, $R/D \rightarrow \infty$ and this finite-sized disk mimics an infinite plate from the perspective of A ; in this case, one analytically recovers $P_{\text{vdW}}^{A\text{-disk}} = -4$, as expected for an atom interacting with an extended (2D) surface [50,51]. This is followed by monotonic decay with D as $R/D \rightarrow 0$ and $P_{\text{vdW}}^{A\text{-disk}} \rightarrow -6$, which is consistent with the well-known asymptotic expression for two finite-sized systems obtained from nonrelativistic quantum mechanics, (i.e., $E_{\text{vdW}} \propto D^{-6}$). From this figure, one immediately sees that the mere presence of a pore fundamentally alters the vdW scaling landscape across all nonasymptotic distances. In the short range, we find that $P_{\text{vdW}} \rightarrow 0$ when $r \neq 0$, as the transverse force on A originating from the vdW interaction with the porous annulus vanishes. The presence of a pore then leads to a markedly slower E_{vdW} decay rate across a wide range (0–40 Å) of distances, with P_{vdW} finally approaching (to $\approx 1\%$) the asymptotic limit of -6 for $D \gtrsim 70 \text{ Å}$. Bound by the limiting cases of $r = 0$ (closed disk) and $r \rightarrow R$ [infinitely thin ring, with $P_{\text{vdW}}^{A\text{-ring}}(R, D) = P_{\text{vdW}}^{A\text{-ann}}(R, R, D) = -6/[1 + (R/D)^2]$], variations in the relative pore size (r/R) and R can be used to tune the extent and length scales over which the system deviates from asymptotic behavior.

Since the inclusion of many-body vdW interactions often leads to power laws with significant deviations from conventional pairwise predictions [37,43,51–55], we now consider how an infinite-order many-body expansion of $E_{\text{vdW}}^{A\text{-ann}}$ would influence the vdW scaling behavior in the presence of a pore. Under the same assumptions, we computed $P_{\text{vdW}}^{A\text{-ann}}$ for the smallest ($r = 1 \text{ Å}$) and largest ($r = R = 10 \text{ Å}$) pore sizes considered above within the random phase approximation (RPA) of the ACFDT (see the Supplemental Material [56]). This approach [63–66] accounts for collective many-body effects and

electrodynamic response screening in the long-range correlation energy, and therefore provides an accurate description of the vdW interaction [53,67–69]. Our ACFDT-RPA results [56] are plotted in Fig. 1 and demonstrate that many-body effects lead to negligible differences in $P_{\text{vdW}}^{A\text{-ann}}$ for D outside of density overlap between A and $\text{ann}[r, R]$, thereby validating a pairwise treatment of this model system for such length scales. We attribute this to the fact that the void space hinders delocalization of the polarizability across the annulus, thereby largely suppressing the influence of many-body effects in $P_{\text{vdW}}^{A\text{-ann}}$.

Next we consider two annuli in a sandwich configuration as a model system for a stacked porous macrocycle dimer (Fig. 2). Under the same assumptions as above, the pairwise $E_{\text{vdW}} = -\sum_{AB} C_6^{AB} R_{AB}^{-6}$ was computed by integrating over the surface elements, $d\sigma_A$ and $d\sigma_B$, located on each annulus, i.e.,

$$E_{\text{vdW}}^{\text{ann-ann}}(r, R, D) = -\frac{C_6^{AB}}{S_A S_B} \int d\sigma_A \int d\sigma_B R_{AB}^{-6}. \quad (3)$$

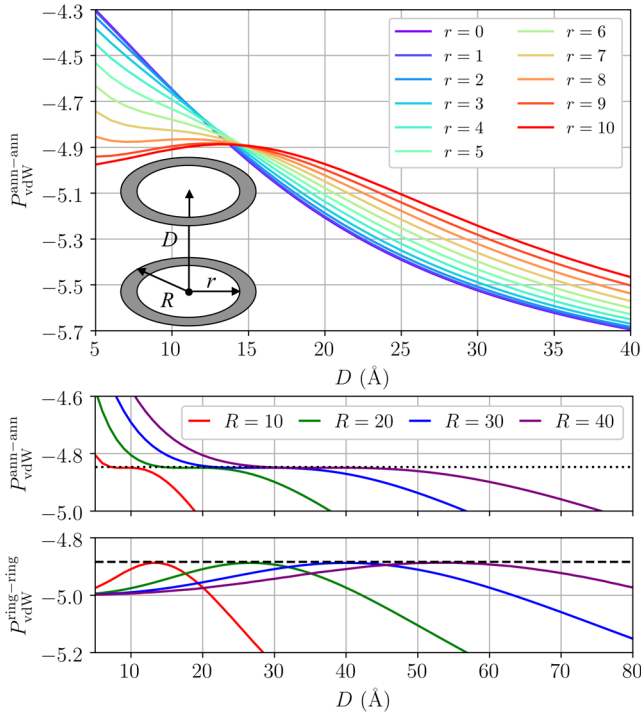


FIG. 2. Top: Effective power law exponents $P_{\text{vdW}}^{\text{ann-ann}}$ for the pairwise vdW interaction between two stacked annuli with $R = 10$ as a function of r and D (all in Å). Depending on the relative pore size, P_{vdW} exhibits widely varying behavior at nonasymptotic distances, ranging from simple monotonic decay (closed disks) to extended plateaus and maxima (rings). Bottom: Extended plateaus (shown here for $R = 10\text{--}40$ Å) occur for annuli with $r/R = 0.75$ at $P_{\text{vdW}} = -4.85$ (dotted line), and correspond to an enhanced vdW interaction across a wide range of intermediate distances. Maxima of $P_{\text{vdW}} = -4.88$ (dashed line) correspond to minima in the E_{vdW} decay rate and occur for rings at a relative distance of $D/R = 1.33$.

This integral can also be evaluated analytically in a cylindrical coordinate system to obtain $P_{\text{vdW}}^{\text{ann-ann}}(r, R, D)$, which is plotted in the top panel of Fig. 2 for two annuli with $R = 10$ Å, and whose general form is given in Ref. [56]. From this figure, one again sees that the presence of a pore leads to non-trivial changes in P_{vdW} across non-asymptotic D ; depending on r/R , P_{vdW} exhibits widely varying behavior, ranging from simple monotonic decay to the formation of extended plateaus and maxima.

In the absence of a pore, $P_{\text{vdW}}^{\text{disk-disk}}(R, D) = -4 - 2/[1 + (R/D)^2]$ has a monotonically decaying form which analytically yields the expected limits of D^{-4} and D^{-6} for short and asymptotic D (*vide supra*). As r increases, radically different behavior emerges with the formation of an extended plateau in P_{vdW} , which corresponds to an enhanced vdW interaction across the intermediate distance range. Mathematically speaking, this plateau results from a stationary point of inflection in P_{vdW} , wherein both $\partial P_{\text{vdW}}/\partial D$ and $\partial^2 P_{\text{vdW}}/\partial D^2$ vanish. These conditions form an underdetermined set of equations that can be analytically solved [56] to yield the relative pore size $r/R = 0.75$ and distance $D/R = 0.91$ at this inflection point. As depicted in the bottom panel of Fig. 2 for two $\text{ann}[0.75R, R]$ with $R = 10\text{--}40$ Å, these plateaus have an analytical value of $P_{\text{vdW}} = -4.85$, and span a remarkably wide range of distances. To approximate the spatial extent of these plateaus, we located the values of D when $P_{\text{vdW}} = -4.85 \pm 0.05$ (a range equivalent to the dotted linewidth) and determined that this enhancement in the vdW interaction persists for $D = 0.45R - 0.55R$. As r increases to the limiting case of two interacting rings, we observe maxima in P_{vdW} , at which point the decay rate of E_{vdW} is minimized. In this case, $P_{\text{vdW}}^{\text{ring-ring}}(R, D) = -5 - 5/[1 + 4(R/D)^2] + 4[1 + 2(R/D)^2]/[1 + 4(R/D)^2 + 6(R/D)^4]$, from which one sees that $P_{\text{vdW}}^{\text{ring-ring}} \rightarrow -5$ in the short range (as $R/D \rightarrow \infty$) and the interaction between these two rings (or 1-spheres) mimics that of two parallel, infinitely long wires (see Fig. 2). At intermediate distances, maxima occur at $D/R = 1.33$ and are bound above by $P_{\text{vdW}} = -4.88$. Since $P_{\text{vdW}}^{\text{ring-ring}}$ is equivalent to that of a point particle A , located directly above the perimeter (not the centroid) of a ring, one can show that these maxima result from the competition between vdW interactions of A with adjacent and distant sectors of the ring.

To investigate the vdW scaling behavior in porous 2D materials, we now consider a model system consisting of periodic layers tiled by hexagons with inner and outer radii, \bar{r} and \bar{R} (denoted by $\text{layer}[\bar{r}, \bar{R}]$). When interacting with a point particle A , numerical evaluation of E_{vdW} [56] shows that $P_{\text{vdW}}^{A\text{-layer}} \rightarrow 0$ in the short range once pores are present in the periodic layer, and $P_{\text{vdW}}^{A\text{-layer}} \rightarrow -4$ in the long range, as expected for A interacting with an infinite 2D surface [50,51]. This short-range behavior is completely analogous

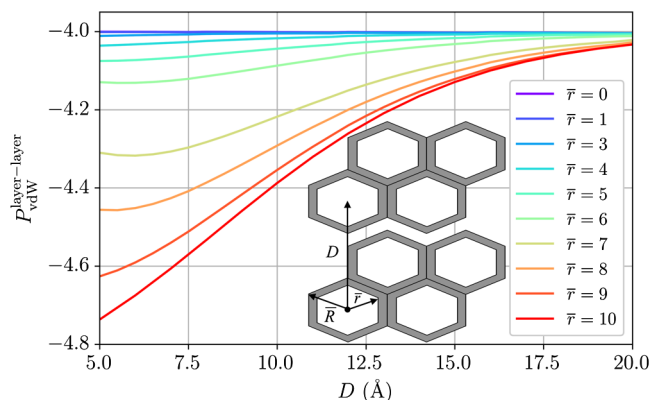


FIG. 3. Effective power law exponents $P_{\text{vdW}}^{\text{layer-layer}}$ for the pairwise vdW interaction between stacked periodic hexagonal bilayers with $\bar{R} = 10$ as a function of \bar{r} and D (all in \AA). When $\bar{r} \neq 0$, such porous 2D materials exhibit fundamentally different behavior (including the formation of minima in P_{vdW}) than the limiting case of two infinite nonporous plates ($\bar{r} = 0$), which has $P_{\text{vdW}} = -4$ for all interlayer separations.

to $P_{\text{vdW}}^{\text{A-ann}}$, which again highlights the difference between porous and nonporous molecules and materials. Numerical results for P_{vdW} in stacked periodic bilayers with $\bar{R} = 10 \text{ \AA}$ are depicted in Fig. 3, where one again sees that the mere presence of a pore leads to remarkably different vdW scaling behavior. As expected for the pairwise vdW interaction between two infinite nonporous plates, $P_{\text{vdW}} = -4$ for all D when $\bar{r} = 0$. In porous 2D materials, however, P_{vdW} strongly depends on \bar{r}/\bar{R} , with larger values leading to markedly slower convergence to this asymptotic limit. In fact, one can even observe minima in P_{vdW} for \bar{r}/\bar{R} values between 0.5 (at $D \approx 0.65\bar{R}$) and 1.0 (at $D \approx 0.20\bar{R}$), at which point the decay rate of E_{vdW} is maximized. In contrast to porous macrocycles, porous bilayer materials *always* have a faster decay rate than their nonporous analogs, and therefore approach asymptotic behavior from below. Not surprisingly, P_{vdW} is also a function of the hexagonal ring size, with larger values of \bar{R} extending the range of nonasymptotic behavior to $D \gtrsim 100 \text{ \AA}$ (e.g., for $\bar{R} = 40 \text{ \AA}$) [56].

To explore how well these models describe the vdW scaling in real porous 2D molecules and materials, we now focus on macrocycle dimers (MC) and periodic bilayers (BL) of three popular COF systems [6–8,48,70,71]: COF-5, TP-COF, and HHTP-DPB COF (Fig. 4). To do so, we compare P_{vdW} from the analytical $\text{ann}[r, R]$ and numerical $\text{layer}[\bar{r}, \bar{R}]$ models with dispersion-inclusive density functional theory (i.e., PBE [72] in conjunction with the effective pairwise TS-vdW approach [73,74]) in QUANTUM ESPRESSO [56,75]. With a range of simple atom-to-atom distance estimates for the inner and outer COF radii, these models provide P_{vdW} values in remarkable agreement with PBE + TS-vdW (Fig. 4, bottom panel). Further optimization of these parameters leads to physical

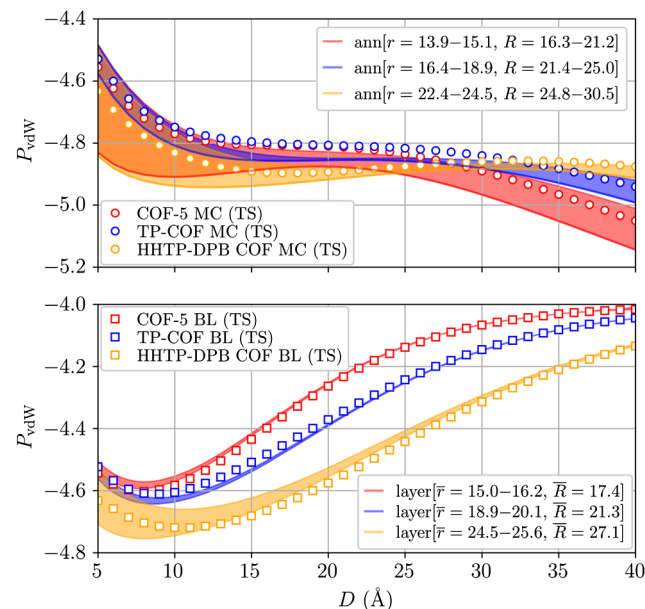
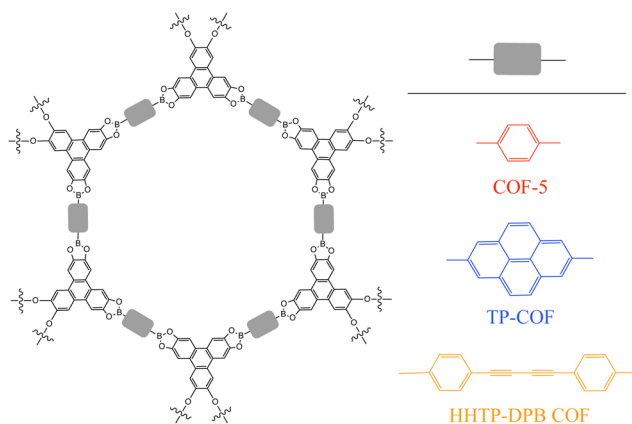


FIG. 4. Top: 2D building blocks for COF-5 (red), TP-COF (blue), and HHTP-DPB COF (orange). In this work, COF macrocycles have capped terminal hydroxyl (-OH) groups. Bottom: Effective power law exponents for stacked COF macrocycle dimers (MC) and periodic bilayers (BL) obtained using the analytical ($\text{ann}[r, R]$) and numerical ($\text{layer}[\bar{r}, \bar{R}]$) models introduced herein (solid lines), and the effective pairwise PBE+TS-vdW approach (TS, circles and squares). $P_{\text{vdW}}^{\text{ann-ann}}$ ($P_{\text{vdW}}^{\text{layer-layer}}$) are provided for a range of r and R (\bar{r} and \bar{R}) based on simple estimates of the COF radii [56], and are in high fidelity with the first-principles based PBE+TS-vdW approach. Quite interestingly, we find that these COF systems have relative pore sizes that lead to characteristic features such as extended plateaus (MC) and minima (BL) in P_{vdW} .

values for r/R (\bar{r}/\bar{R}) of 0.72 (0.88), 0.75 (0.88), and 0.81 (0.93), for COF-5, TP-COF, and HHTP-DPB COF, respectively; these values are essentially contained in the ranges estimated above and yield even better agreement between the curves [56]. Interestingly, these values are in the neighborhood of $r/R = 0.75$, which corresponds to the stationary point of inflection in $P_{\text{vdW}}^{\text{ann-ann}}$; as such, COF macrocycle dimers are characterized by P_{vdW} that

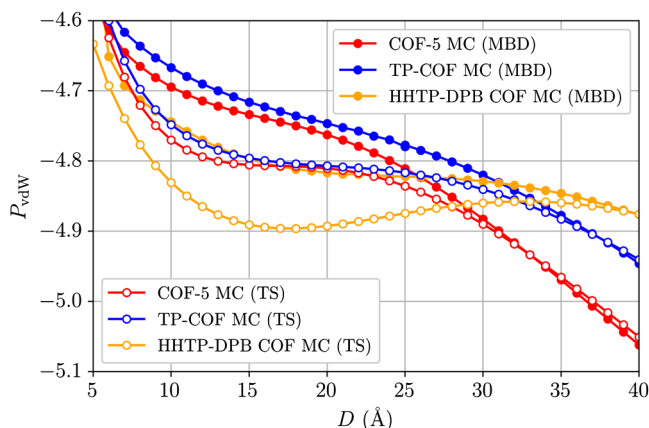


FIG. 5. Effective power law exponents for COF macrocycle dimers (MC) when accounting for pairwise (TS, open circles) and many-body (MBD, closed circles) vdW interactions.

exhibit extended plateaus across a range of distances ($D \approx 10\text{--}40$ Å) quite relevant to the nanoscale. For the bilayers, we also find characteristic minima in P_{vdW} at $D \approx 7\text{--}10$ Å, where the decay rate of E_{vdW} has peaked.

In analogy to the ACFDT-RPA treatment of the A -ann model system above, we employed the many-body dispersion (MBD) model [67,68,76–78] in conjunction with PBE to investigate how higher-order vdW interactions might influence the scaling behavior in COF macrocycle dimers. As depicted in Fig. 5, we find that these relatively short-ranged and anisotropic interactions lead to some deviations in P_{vdW} at small or intermediate distances, and converge to pairwise behavior for $D \gtrsim 30\text{--}35$ Å. Of greater interest here is the fact that the extended plateaus in P_{vdW} are robust features of the vdW scaling landscape, with many-body effects actually enhancing P_{vdW} for $D = 10\text{--}30$ Å, a range of distances quite relevant to COF self-assembly [48,49].

The unique vdW scaling behavior originating from the void space present in porous 2D molecules and materials provides new insight into the self-assembly and design of complex nanostructures. For stacked macrocycle dimers, plateaus and maxima in P_{vdW} demonstrate that a range of relative pore sizes lead to a nontrivial interplay between P_{vdW} , which favors small (large) pores in the short (long) range, and $E_{\text{vdW}}/\text{atom}$, which favors small pores for all D . In extended systems, however, P_{vdW} and $E_{\text{vdW}}/\text{atom}$ work in tandem across all interlayer distances, collectively biasing the number of layers preferred in a 2D material. Since the onset and extent of these effects are governed by r and R (or \bar{r} and \bar{R}), these quantities can be leveraged to influence the self-assembly of complex porous nanostructures ranging from stacked macrocycles to multilayered COF architectures.

All authors thank Greg Ezra, Jan Hermann, Hsin-Yu Ko, and Alexandre Tkatchenko for critically reading the

manuscript. This work was partially supported by start-up funds from Cornell University and the Cornell Center for Materials Research (CCMR) with funding from the National Science Foundation MRSEC program (DMR-1719875). This research used resources of the National Energy Research Scientific Computing Center, which is supported by the Office of Science of the U.S. Department of Energy under Contract No. DE-AC02-05CH11231.

*distasio@cornell.edu

- [1] K. S. Novoselov, D. Jiang, F. Schedin, T. J. Booth, V. V. Khotkevich, S. V. Morozov, and A. K. Geim, *Proc. Natl. Acad. Sci. U.S.A.* **102**, 10451 (2005).
- [2] K. S. Novoselov, S. V. Morozov, T. M. G. Mohinddin, L. A. Ponomarenko, D. C. Elias, R. Yang, I. I. Barbolina, P. Blake, T. J. Booth, D. Jiang, J. Giesbers, E. W. Hill, and A. K. Geim, *Phys. Status Solidi B* **244**, 4106 (2007).
- [3] C. Zhi, Y. Bando, C. Tang, H. Kuwahara, and D. Golberg, *Adv. Mater.* **21**, 2889 (2009).
- [4] A. A. Balandin, *Nat. Mater.* **10**, 569 (2011).
- [5] R. Mas-Ballesté, C. Gómez-Navarro, J. Gómez-Herrero, and F. Zamora, *Nanoscale* **3**, 20 (2011).
- [6] A. P. Côté, A. I. Benin, N. W. Ockwig, M. O’Keeffe, A. J. Matzger, and O. M. Yaghi, *Science* **310**, 1166 (2005).
- [7] A. P. Côté, H. M. El-Kaderi, H. Furukawa, J. R. Hunt, and O. M. Yaghi, *J. Am. Chem. Soc.* **129**, 12914 (2007).
- [8] E. L. Spitler and W. R. Dichtel, *Nat. Chem.* **2**, 672 (2010).
- [9] A. Nagai, Z. Guo, X. Feng, S. Jin, X. Chen, X. Din, and D. Jiang, *Nat. Commun.* **2**, 536 (2011).
- [10] X. X. Feng, X. Ding, and D. Jiang, *Chem. Soc. Rev.* **41**, 6010 (2012).
- [11] S. Ding and W. Wang, *Chem. Soc. Rev.* **42**, 548 (2013).
- [12] C. S. Diercks and O. M. Yaghi, *Science* **355**, eaal1585 (2017).
- [13] H. Li, M. Eddaoudi, M. O’Keeffe, and O. M. Yaghi, *Nature (London)* **402**, 276 (1999).
- [14] S. L. James, *Chem. Soc. Rev.* **32**, 276 (2003).
- [15] D. Wu, F. Xu, B. Sun, R. Fu, H. He, and K. Matyjaszewski, *Chem. Rev.* **112**, 3959 (2012).
- [16] S. Kitagawa, R. Kitaura, and S. Noro, *Angew. Chem., Int. Ed. Engl.* **43**, 2334 (2004).
- [17] S. Wan, J. Guo, J. Kim, H. Ihee, and D. Jiang, *Angew. Chem., Int. Ed. Engl.* **48**, 5439 (2009).
- [18] H. Song, J. J. Wu, H. Cheng, and F. Kang, *Joule* **2**, 442 (2018).
- [19] T. Liu, J. Ding, Z. Su, and G. Wei, *Mater. Today Energy* **6**, 79 (2017).
- [20] R. W. Tilford, S. J. Mugavero, P. J. Pellechia, and J. J. Lavigne, *Adv. Mater.* **20**, 2741 (2008).
- [21] J. Lee, O. K. Farha, J. Roberts, K. A. Scheidt, S. T. Nguyen, and J. T. Hupp, *Chem. Soc. Rev.* **38**, 1450 (2009).
- [22] M. Vallet-Regí, F. Balas, and D. Arcos, *Angew. Chem., Int. Ed. Engl.* **46**, 7548 (2007).
- [23] D. Chimene, D. L. Alge, and A. K. Gaharwar, *Adv. Mater.* **27**, 7261 (2015).
- [24] S. Xie, L. Tu, Y. Han, L. Huang, K. Kang, K. U. Lao, P. Poddar, C. Park, D. A. Muller, R. A. DiStasio, Jr., and J. Park, *Science* **359**, 1131 (2018).

- [25] L. A. Ponomarenko, A. K. Geim, A. A. Zhukov, R. Jalil, S. V. Morozov, K. S. Novoselov, I. V. Grigorieva, E. H. Hill, V. V. Cheianov, V. I. Fal'Ko, K. Watanabe, T. Taniguchi, and R. V. Gorbachev, *Nat. Phys.* **7**, 958 (2011).
- [26] S. J. Haigh, A. Gholinia, R. Jalil, S. Romani, L. Britnell, D. C. Elias, K. S. Novoselov, L. A. Ponomarenko, A. K. Geim, and R. Gorbachev, *Nat. Mater.* **11**, 764 (2012).
- [27] A. K. Geim and I. V. Grigorieva, *Nature (London)* **499**, 419 (2013).
- [28] K. S. Novoselov, A. Mishchenko, A. Carvalho, and A. H. C. Neto, *Science* **353**, aac9439 (2016).
- [29] D. Langbein, *Theory of van der Waals Attraction* (Springer, Berlin, 1974).
- [30] V. A. Parsegian, *van der Waals Forces: A Handbook for Biologists, Chemists, Engineers, and Physicists* (Cambridge University Press, Cambridge, England, 2005).
- [31] I. G. Kaplan, *Intermolecular Interactions: Physical Picture, Computational Methods and Model Potentials* (Wiley, New York, 2006).
- [32] A. J. Stone, *The Theory of Intermolecular Forces*, 2nd ed. (Oxford University Press, Oxford, 2013).
- [33] J. L. Beeby, *J. Phys. C* **4**, L359 (1971).
- [34] P. Loskill, H. Hähl, T. Faidt, S. Grandthyll, F. Müller, and K. Jacobs, *Adv. Colloid Interface Sci.* **179**, 107 (2012).
- [35] P. Loskill, J. Puthoff, M. Wilkinson, K. Mecke, K. Jacobs, and K. Autumn, *J. R. Soc. Interface* **10**, 20120587 (2013).
- [36] V. V. Gobre and A. Tkatchenko, *Nat. Commun.* **4**, 2341 (2013).
- [37] A. Ambrosetti, N. Ferri, R. A. DiStasio, Jr., and A. Tkatchenko, *Science* **351**, 1171 (2016).
- [38] T. Gould, K. Simpkins, and J. F. Dobson, *Phys. Rev. B* **77**, 165134 (2008).
- [39] L. Spanu, S. Sorella, and G. Galli, *Phys. Rev. Lett.* **103**, 196401 (2009).
- [40] Y. J. Dappe, J. Ortega, and F. Flores, *Phys. Rev. B* **79**, 165409 (2009).
- [41] S. Lebègue, J. Harl, T. Gould, J. G. Ángyán, G. Kresse, and J. F. Dobson, *Phys. Rev. Lett.* **105**, 196401 (2010).
- [42] A. J. Misquitta, J. Spencer, A. J. Stone, and A. Alavi, *Phys. Rev. B* **82**, 075312 (2010).
- [43] A. J. Misquitta, R. Maezono, N. D. Drummond, A. J. Stone, and R. J. Needs, *Phys. Rev. B* **89**, 045140 (2014).
- [44] K. A. Makhnovets and A. K. Kolezhuk, *Phys. Rev. B* **96**, 125427 (2017).
- [45] P. S. Venkataram, J. Hermann, A. Tkatchenko, and A. W. Rodriguez, *Phys. Rev. Lett.* **118**, 266802 (2017).
- [46] J. F. Dobson, A. White, and A. Rubio, *Phys. Rev. Lett.* **96**, 073201 (2006).
- [47] T. Gould, E. Gray, and J. F. Dobson, *Phys. Rev. B* **79**, 113402 (2009).
- [48] A. D. Chavez, B. J. Smith, M. K. Smith, P. A. Beaucage, B. H. Northrop, and W. R. Dichtel, *Chem. Mater.* **28**, 4884 (2016).
- [49] D. N. Buncck and W. R. Dichtel, *J. Am. Chem. Soc.* **135**, 14952 (2013).
- [50] A. M. C. Reyes and C. Eberlein, *Phys. Rev. A* **80**, 032901 (2009).
- [51] A. Ambrosetti, P. L. Silvestrelli, and A. Tkatchenko, *Phys. Rev. B* **95**, 235417 (2017).
- [52] H. Kim, J. O. Sofo, D. Velegol, M. W. Cole, and A. A. Lucas, *Langmuir* **23**, 1735 (2007).
- [53] J. F. Dobson, *Int. J. Quantum Chem.* **114**, 1157 (2014).
- [54] J. F. Dobson, T. Gould, and G. Vignale, *Phys. Rev. X* **4**, 021040 (2014).
- [55] C. A. S. Batista, R. G. Larson, and N. A. Kotov, *Science* **350**, 1242477 (2015).
- [56] See Supplemental Material at <http://link.aps.org/supplemental/10.1103/PhysRevLett.122.026001> for more details regarding the computation of the many-body dispersion energy from the Adiabatic-Connection Fluctuation-Dissipation Theorem, analytical determination of the stationary point of inflection in $P_{\text{vdW}}^{\text{ann-ann}}(r, R, D)$, numerical evaluation of E_{vdW} in periodic bilayers, computational details of the vdW interactions in COF systems, as well as selection and optimization of the inner and outer COF radii, which includes Refs. [57–62].
- [57] J. F. Dobson, K. McLennan, A. Rubio, J. Wang, T. Gould, H. M. Le, and B. P. Dinte, *Aust. J. Chem.* **54**, 513 (2001).
- [58] X. Ren, P. Rinke, C. Joas, and M. Scheffler, *J. Mater. Sci.* **47**, 7447 (2012).
- [59] D. Lu, H. Nguyen, and G. Galli, *J. Chem. Phys.* **133**, 154110 (2010).
- [60] J. F. Dobson, *Topics in Condensed Matter Physics* (Nova, New York, 1994).
- [61] A. Mayer, *Phys. Rev. B* **75**, 045407 (2007).
- [62] X. Chu and A. Dalgarno, *J. Chem. Phys.* **121**, 4083 (2004).
- [63] D. Bohm and D. Pines, *Phys. Rev.* **92**, 609 (1953).
- [64] M. Gell-Mann and K. A. Brueckner, *Phys. Rev.* **106**, 364 (1957).
- [65] O. Gunnarsson and B. I. Lundqvist, *Phys. Rev. B* **13**, 4274 (1976).
- [66] D. C. Langreth and J. P. Perdew, *Phys. Rev. B* **15**, 2884 (1977).
- [67] R. A. DiStasio, Jr., V. V. Gobre, and A. Tkatchenko, *J. Phys. Condens. Matter* **26**, 213202 (2014).
- [68] A. Ambrosetti, A. M. Reilly, R. A. DiStasio Jr., and A. Tkatchenko, *J. Chem. Phys.* **140**, 18A508 (2014).
- [69] J. Hermann, R. A. DiStasio, Jr., and A. Tkatchenko, *Chem. Rev.* **117**, 4714 (2017).
- [70] S. Wan, J. Guo, J. Kim, H. Ihee, and D. Jiang, *Angew. Chem., Int. Ed. Engl.* **120**, 8958 (2008).
- [71] E. L. Spitler, B. T. Koo, J. L. Novotney, J. W. Colson, F. J. Uribe-Romo, G. D. Gutierrez, P. Clancy, and W. R. Dichtel, *J. Am. Chem. Soc.* **133**, 19416 (2011).
- [72] J. P. Perdew, K. Burke, and M. Ernzerhof, *Phys. Rev. Lett.* **77**, 3865 (1996).
- [73] A. Tkatchenko and M. Scheffler, *Phys. Rev. Lett.* **102**, 073005 (2009).
- [74] N. Ferri, R. A. DiStasio, Jr., A. Ambrosetti, R. Car, and A. Tkatchenko, *Phys. Rev. Lett.* **114**, 176802 (2015).
- [75] P. Giannozzi *et al.*, *J. Phys. Condens. Matter* **29**, 465901 (2017).
- [76] A. Tkatchenko, R. A. DiStasio, Jr., R. Car, and M. Scheffler, *Phys. Rev. Lett.* **108**, 236402 (2012).
- [77] R. A. DiStasio, Jr., O. A. von Lilienfeld, and A. Tkatchenko, *Proc. Natl. Acad. Sci. U.S.A.* **109**, 14791 (2012).
- [78] M. A. Blood-Forsythe, T. Markovich, R. A. DiStasio, Jr., R. Car, and A. Aspuru-Guzik, *Chem. Sci.* **7**, 1712 (2016).